Astron. Astrophys. 358, 1133–1141 (2000)

ASTRONOMY AND ASTROPHYSICS

ISO results on bright Main Belt asteroids: PHT–S observations⋆

E. Dotto[1,2], T.G. Müller[3], M.A. Barucci[1], Th. Encrenaz[1], R.F. Knacke[4], E. Lellouch[1], A. Doressoundiram[1], J. Crovisier[5], J.R. Brucato[6], L. Colangeli[6], and V. Mennella[6]

[1] DESPA – Observatoire de Paris, 92195 Meudon, France
[2] Osservatorio Astronomico di Torino, Italy
[3] ISO Data Centre, ESA Astrophysics Division, Villafranca, Spain
[4] Penn. State University, Erie, PA, USA
[5] ARPEGES – Observatoire de Paris, 92195 Meudon, France
[6] Osservatorio Astronomico di Capodimonte, Italy

Received 22 June 1999 / Accepted 27 March 2000

Abstract. Observations of asteroids have been performed by the ISO satellite with PHT–S. The aim of these observations was to investigate the physical and compositional properties of five bright Main Belt Asteroids (1 Ceres, 2 Pallas, 3 Juno, 4 Vesta, and 52 Europa) in the spectral range 5.8–11.6 μm. The Standard Thermal Model and a black-body fit have been applied to the obtained spectra to derive sub-solar and black-body temperatures. An advanced Thermo-Physical Model has been applied to model the thermal continuum. In order to better interpret the observed spectral features, we compared the ISO data with meteorite and mineral spectra available in literature and with spectra of a selected number of minerals obtained in laboratory. The spectral behaviour of all the observed asteroids from 8 to 11 μm suggest the presence of silicates on the surfaces.

Key words: techniques: spectroscopic – minor planets, asteroids – infrared: solar system – ISO – Asteroid Individual: 1 Ceres, 2 Pallas, 3 Juno, 4 Vesta, 52 Europa

1. Introduction

The Infrared Space Observatory (ISO), an ESA project, was launched in November 1995 and has been operative until April 1998 (Kessler et al. 1996). Among various instruments on board ISO, we used the imaging photopolarimeter ISOPHOT (Lemke et al. 1996) and in particular the subsystem PHT–S which consists of two low-resolution grating spectrometers which cover the wavelength ranges 2.5–4.9 μm (PHT–SS) and 5.8–11.6 μm (PHT–SL). PHT–SS and PHT–SL have a common square entrance aperture of 24 × 24 arcsec. The resolution $\lambda/\Delta\lambda$ is about 85 for PHT–SS and about 95 for PHT–SL.

Send offprint requests to: E. Dotto, Osservatorio Astronomico di Torino, Strada Osservatorio 20, 10025 Pino Torinese (TO), Italy (dotto@to.astro.it)

⋆ Based on observations with ISO, an ESA project with instruments funded by ESA Member States (especially the PI countries: France, Germany, the Netherlands and the United Kingdom) with the participation of ISAS and NASA.

Table 1. Aspect data of the ISO observations with PHT–S

Object	Obs. date	Start time (UT)	Integ. time (sec)	Δ (AU)	r (AU)	α (deg)
1 Ceres	14/05/97	10:53:43	64	2.97	3.02	19.4
2 Pallas	12/04/97	04:39:08	64	3.30	3.32	17.4
3 Juno	07/12/96	23:58:47	256	1.43	2.01	27.2
4 Vesta	13/06/97	13:57:53	64	2.56	2.37	23.3
52 Europa	16/11/97	17:02:49	256	2.68	3.17	17.0

Most of the infrared wavelength range is not accessible from the ground and as a matter of fact is still poorly known for asteroids. The InfraRed Astronomical Satellite (IRAS) performed a survey of more than 1800 asteroids at four wavelengths (12, 25, 60 and 100 μm), allowing us to evaluate their albedo and diameter (Tedesco et al. 1992). A few infrared spectra on asteroids come from the NASA Ames HIFOGS spectrometer (Witteborn et al. 1995), working on the Kuiper Airborne Observatory (KAO), which covered the 5–14 μm range (Cohen et al. 1998).

In order to increase the available infrared data set on asteroids, to study their spectral properties at these wavelengths and to investigate their possible surface composition, several ISO programs have been devoted to the observation of these objects (e.g. Barucci et al. 1997; Dotto et al. 1999). In this paper we present observations, up to 11.6 μm, concerning five bright main belt asteroids (1 Ceres, 2 Pallas, 3 Juno, 4 Vesta, 52 Europa) included in the central program "Observations of Galilean satellites and asteroids with ISO".

2. Observations and data reduction

The observations of asteroids presented here have been carried out with PHT–S between Dec. 1996 and Nov. 1997. In Table 1 the observational date and time, and the aspect data (heliocentric distance r, geocentric distance Δ and phase angle α) of the observed asteroids are listed. The observations have been performed in staring mode with a default of 32 sec dark expo-

sure at the beginning of the measurement. ISOPHOT Interactive Analysis (PIA[1]) V7.3.3 was used for the standard data reduction up to signal level, including linear ramp fitting, deglitching on ramp and signal level and orbit dependent dark signal subtraction (Gabriel et al. 1997). We used the *dynamic calibration* procedure, where the time evolution of each individual pixel signal is compared with calibration measurements which best match this signal level. The dynamic calibration of PHT–S includes 24 well-known stellar calibration standards (Acosta, private communication, 1999). The model spectra are based on Hammersley et al. (1998). The model spectra of a few late type K and M giants are provided by M. Cohen, based on Cohen et al. (1999) and references therein, including the fundamental bands of CO and SiO (Cohen et al. 1992). We used 2 calibration standards for each detector pixel, which are then combined by weighting the ratios between target and calibrator signals. The presented observations have been carried out without considering the background contribution. We calculated a maximal background effect of 2% for the faintest asteroid Europa and of less than 1% for the others, which is negligible in view of calibration uncertainties.

The PHT–SS 2.5–4.9 μm part of the asteroid spectra is at a very low flux level, often close to the detection limit. This part covers the transition range between reflected sunlight and thermal emission, which is usually not included in thermal modelling programs. Therefore we exclude in this paper this part of the spectrum.

The uncertainties from the signal processing by PIA are 3–5%, which reflect also the relative accuracy from pixel to pixel. The absolute uncertainty is generally stated better than 30% (Klaas et al., 1997). Since we used an interactive analysis with improved calibration we believe that the absolute calibration is better than 15%. This is also in agreement with our cross-calibration experiences between different ISO instruments and with reliable source models. In cases where late type K and M giants are used for calibration, an additional error source, coming from the CO and SiO line modelling, has to be considered.

In Fig. 1 the low-resolution spectra between 5.8 and 11.6 μm are shown with the uncertainties produced by the signal processing procedure. During the observation of 1 Ceres the detector temperature was outside the nominal range of 2.8–3.1 K, resulting in some problems in the 5–7 μm range, where the detector pixels seem to show a different signal transient behaviour. For this reason only the 7.8–11.6 μm part of the spectrum of this asteroid has been taken into account.

3. Models

The emission of asteroids beyond $\sim 5\,\mu$m is dominated by radiation thermally emitted from their surface. A black-body fit and the Standard Thermal Model (STM) have been applied to the obtained infrared spectra to determine the range of surface (black-body and sub-solar) temperatures. To investigate in a detailed way the spectral features we applied a more sophisticated Thermo-Physical Model (TPM).

[1] PIA is a joint development by the ESA Astrophysics Division and the ISOPHOT consortium.

Table 2. Computed temperatures

Object	Black-body temp. (K)	Sub-solar temp. (K)
1 Ceres	215	247
2 Pallas	204	235
3 Juno	248	295
4 Vesta	224	266
52 Europa	207	242

3.1. Black-body and sub-solar temperatures

To determine the black-body temperature of the observed asteroids we fitted the 5.8–11.6 μm part of the infrared spectra with a Planck function multiplied by the solid angle of the objects. Both the solid angle and the black-body temperature were treated as free parameters. This procedure provided diameters in close agreement (to within 8%) with the known values of the effective diameters of these objects. This small discrepancy is not surprising given the calibration uncertainties. The values of the temperature are reported in Table 2.

The sub-solar temperature of the observed objects was computed by applying the Standard Thermal Model. A review of the model and its history is given by Lebofsky & Spencer (1989, and references therein). The STM has been used by Tedesco et al. (1992) in the IRAS asteroid survey. It assumes a non-rotating spherical asteroid, in instantaneous equilibrium with solar insolation, observed at 0° solar phase angle. In this ideal situation, in which the thermal inertia is neglected, and the asteroid nightside emission is thus not taken into account, the sub-solar temperature is given as:

$$T_{SS} = \left[\frac{(1-A)S}{\eta\epsilon\sigma}\right]^{1/4} \text{and } T(\Omega) = T_{SS}\cos^{1/4}(\Omega) \qquad (1)$$

where Ω is the solar zenith angle, A is the bolometric Bond albedo, S is the solar flux at the distance of the asteroid, η (infrared beaming) is an empirical factor adjusted so that the model matches the integrated flux of the object at a given wavelength, ϵ is the wavelength-independent emissivity and σ is the Stefan-Boltzmann constant. The values of the sub-solar temperature obtained applying the STM to our observations (from Eq. 1 and the data in Table 3) are listed in Table 2.

In this simplified model the infrared beaming and the phase angle geometry are empirically corrected, generally with correction factors of η = 0.756 and 0.01 mag deg^{-1}, respectively (see Lebofsky & Spencer 1989).

In reality as the thermal inertia is not zero, some energy is emitted on the nightside of the asteroid. For realistic thermal inertias and typical rotation periods of 5 to 10 hours, this energy loss can be up to 30% depending on the wavelength, the asteroid's spin vector and the observing geometry (Müller,

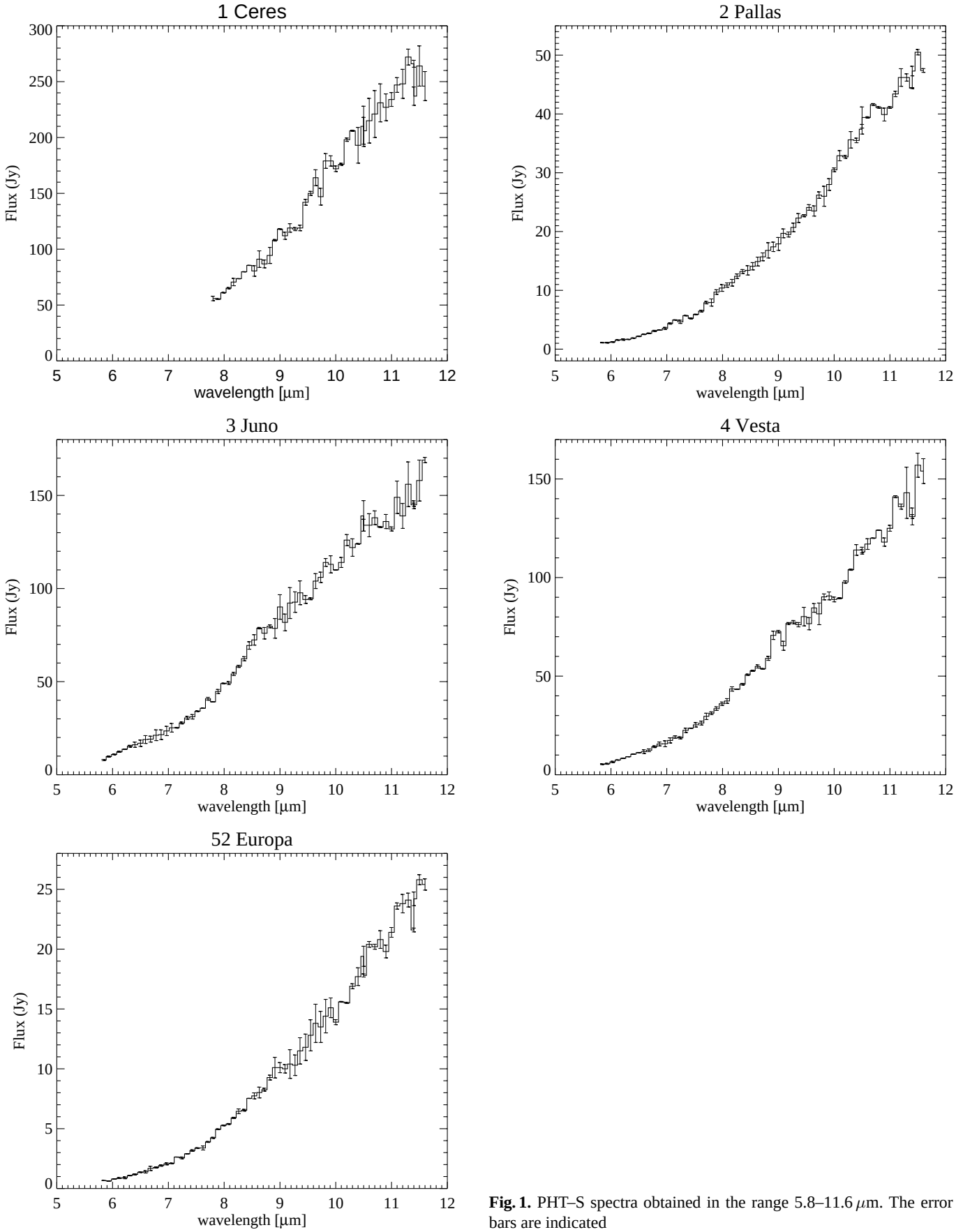

Fig. 1. PHT–S spectra obtained in the range 5.8–11.6 μm. The error bars are indicated

Table 3. TPM input parameters

Object	G	p_v	$2a$ (km)	a/b	b/c	λ_p (deg)	β_p (deg)	P_{sid} (day)	γ_o (deg)	JD_o	ref.
1 Ceres	0.09	0.104	959.2	1.00	1.06	332	+70	0.3780910	86	2440587.5	(i)
2 Pallas	0.08	0.168	574.0	1.06	1.05	45	–15	0.32555136	81	2440587.5	(ii)
3 Juno	0.31	0.241	291.3	1.21	1.20	108	+36	0.300397	5	2440587.5	(iii)
4 Vesta	0.34	0.339	578.0	1.03	1.22	319	+59	0.2225887	344	2440587.5	(iv)
52 Europa	–0.004	0.058	364.0	1.20	1.21	70	+12	0.2344717	59	2446251.5	(v)

(i) G from Müller & Lagerros (1998). Diameter and shape determined from occultation observations combined with high resolution measurements and extensive photoelectric photometry (Millis et al. 1987; Saint-Pé et al. 1993; Merline et al. 1996; Drummond et al. 1998).
(ii) G and $2a$-value from Müller & Lagerros (1998) and spin vector Magnusson (1986) and Erikson (priv. com.)
(iii) by Müller & Lagerros (1998)
(iv) by Müller & Lagerros (1998), Thomas et al. (1997a) and Drummond et al. (1998).
(v) spin vector from Erikson (priv. com.) $2a$-value and albedo from IRAS, G from Michalowski et al. (1995)

1997). Nonetheless, the STM is very useful for a first estimation of albedo and diameter parameters. It is admittedly of little interest for well-known asteroids.

3.2. Thermo-physical model

The five asteroids presented here are among the brightest and the best known objects in the Main Belt: their spin vector, shape and size have been computed with good precision on the basis of occultation data and extensive photometric observations. For Ceres and Vesta additional information is available from Hubble Space Telescope (HST) observations (see references in Table 3). For this reason, to model the thermal continuum of these objects, we applied the Thermo-Physical Model developed by Lagerros (1996, 1997, 1998) and already used and refined by Müller & Lagerros (1998). In these references a detailed description of the model, including discussions of the individual parameters and their possible values, can be found.

In essence, the TPM calculates the surface temperature from the energy balance between absorbed solar radiation, the thermal emission, and heat conduction into the surface material. The disk integrated model flux at the wavelength λ is

$$F_\lambda = \frac{1}{\pi\Delta^2} \oint_S \epsilon_d B_\lambda(\gamma T)\mu \, dS, \qquad (2)$$

where Δ is the distance to the observer, B_λ the Planck function, and the direction cosine μ projects the surface element dS towards the observer. The "beaming function" γ, and the wavelength- and direction-dependent emissivity ϵ_d are discussed in Müller & Lagerros (1998).

All objects are described as rotating ellipsoids. The bolometric albedo is deduced from the slope parameter G and the geometric albedo p_V. Here we use a grey model hemispherical emissivity ϵ_h (which is the integral over the hemisphere of ϵ_d) of 1.0. Since ϵ_d, and therefore also ϵ_h, is tied to the volume single-scattering albedo, it allows us to interpret the flux ratio (observation divided by model) as the observed wavelength-dependent emissivity, which characterizes the surface material. The values for thermal inertia are taken from Müller et al. (1999) and Müller & Lagerros (1998), with a default of $\Gamma = 15\,\mathrm{J\,m^{-2}\,s^{-0.5}\,K^{-1}}$ for 52 Europa. A redetermination of Γ from PHT–S data alone was not possible, since there is only one PHT–S measurement, either before or after opposition. Therefore the asymmetry due to the morning/afternoon temperatures at the terminator could not be investigated.

It was shown in Müller & Lagerros (1998) that the idea to model the IR beaming by f, the fraction of the surface covered by craters, and ρ, the r.m.s. of the surface slopes, worked fine on a large sample of observations. However a determination of ρ and f was not possible here due to the lack of data. The beaming parameters ρ and f are so far determined with high accuracy only for 1 Ceres (Müller et al. 1999). Discussion about the "Thermal Infrared Beaming" can be found in Lagerros (1998) and in Jämsä et al. (1993) who found a ρ value of 0.4 for the Moon. Fig. 2 shows the ratio between the observed KAO fluxes of Ceres (Cohen et al. 1998) and the TPM predictions (noted "OBS/MOD"), corresponding to different values of ρ and f. From the physical point of view this means to consider different surface roughness/structures/porosity. As shown in Fig. 2 a change in these two parameters causes a change of slope of the curve. An increase in surface roughness produces an enhanced beaming effect with a stronger peak emission and therefore a steeper slope in the Wien-part of the spectral energy distribution in the observed/modelled ratio. For the five asteroids considered here, we have kept the Ceres beaming values of ρ = 0.7 and f = 0.6 based on ISO-Short Wavelength Spectrometer (SWS) observations of Ceres (Müller et al. 1999). This choice might slightly influence the overall slope of the observed/modelled ratio and therefore the appearance of the spectral features, but the amount of available data is not sufficient for a detailed determination of ρ and f.

4. Discussion

Using the TPM we calculated the thermal emission at the time of ISO observations for all of the observed asteroids considering the G value, albedo, $2a$-value, semimajor axes a/b and b/c, pole coordinates, sidereal period, absolute rotational phase and zero point time as given in Table 3. Then we divided the observed spectrum by the TPM (expected) flux in order to search for

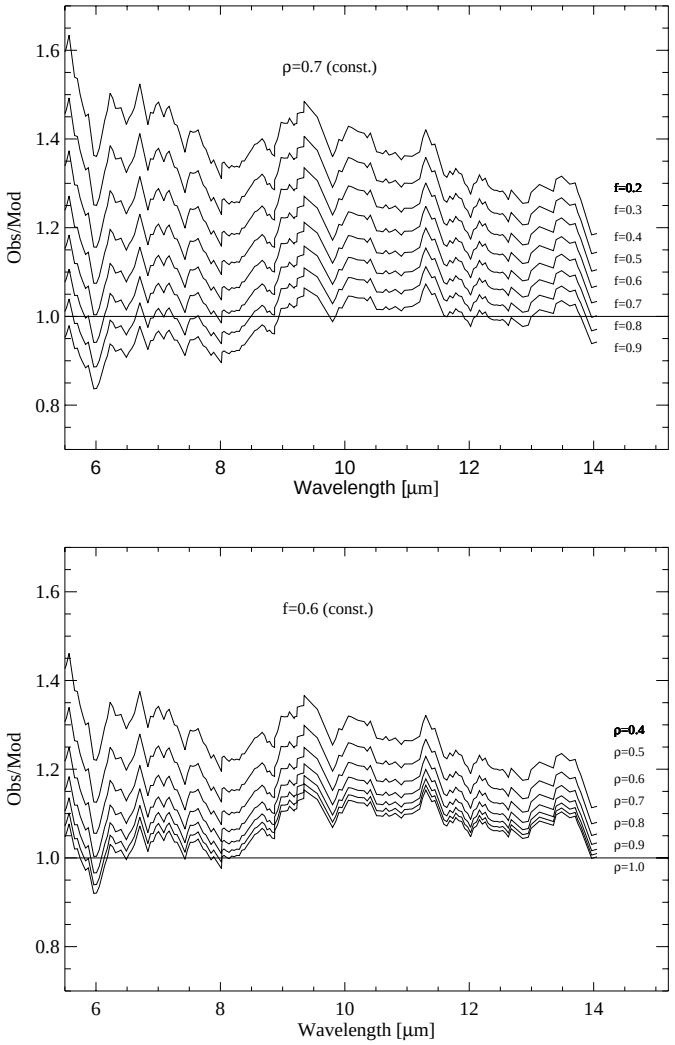

Fig. 2. The influence of the beaming model parameters ρ and f. Top: with a constant r.m.s. of the surface slopes ($\rho = 0.7$) the fraction f of the surface coverage by craters has been varied from 20 to 90 % of the total surface. A higher f-value increases the model flux (smaller ratio OBS/MOD) and makes the predicted flux in this wavelength range steeper. Bottom: with a constant surface coverage by craters ($f = 0.6$) the r.m.s. of the surface slopes ρ is varied from 0.4 to 1.0. A higher ρ-value increases the model flux (smaller ratio OBS/MOD) and makes the predicted flux in this wavelength range steeper. In this figure the observations are the KAO data of 1 Ceres

spectral features superimposed to the thermal emission continuum. In general, the TPM produced absolute flux in agreement with the observed values within their calibration uncertainties. Because we are primarily interested in spectral variations of the emissivity, we scaled the observation to model ratios in a way that the maximum emissivity is equal to 1.0. The resulting spectra are noted "Relative OBS/MOD".

The interpretation of the obtained spectral features is neither easy nor unique. In fact asteroid spectra are affected, not only by the chemical composition of the surfaces, but also by several unknown physical parameters, such as density, particle size and packing. Moreover asteroid surfaces are composed of mixtures

Table 4. Minerals analyzed in the laboratory

Phyllosilicate:	Kaolinite
Quartz	
Opal	
Serpentinite	
Oxide:	Hematite
Hydroxide:	Goethite
Pyroxene 1:	Enstatite
Pyroxene 2:	Jadeite
Pyroxene 3:	Augite
Olivine:	Forsterite
Mica:	Muscovite

of minerals, whose absorption features are combined following non-linear paths. The mixing model for coarse particulate minerals is linear, at least in the reststrahlen region (Thompson & Salisbury 1993), while at smaller particle dimensions, volume scattering becomes important and consequently the mixing model becomes non-linear (Salisbury & Wald 1992). Ground-based and space observations indicate that asteroid surfaces are covered by regolith. Therefore, the best way to interpret the asteroid spectra and to infer some information on the surface composition of the observed bodies, is to analyze all the spectral features on the basis of mid-infrared spectra of powdered meteorites and minerals.

In the spectral range considered in this paper, the most diagnostic feature is the Christiansen peak which marks the boundary between the wavelength region dominated by volume scattering (around 2.5–7.5 μm) and the wavelength region dominated by surface scattering and reststrahlen bands (around 8.5–11.5 μm).

In order to interpret our ISO spectra of asteroids, first we compare their spectral features with those of powdered stony meteorites and minerals available in literature (Salisbury et al. 1991a,b; ASTER spectral library on http://speclib.jpl.nasa.gov) and we combined these inputs with all the information obtained about each asteroid from independent, shorter-wavelength observations. Then, a selected number of mineral samples has been chosen and laboratory experiments have been performed at different grain sizes.

4.1. Laboratory experiments

The materials analyzed in this work belong to different classes of minerals and are listed in Table 4. In order to obtain particulate samples we ground bulk materials in an agata mill. The size distribution of grains was studied by Field Emission Scanning Electron Microscopy (FESEM - mod. Stereoscan FE360) with a spatial resolution of 2 nm. To prepare samples for FESEM analysis a solution of dust grains and ethanol was deposited onto a silicon wafer chip fixed on an aluminium stub. The grain sizes range from tenths to few tens of microns. FESEM images revealed that submicron particles usually stick onto larger ones. Small grain size are appropriate for comparison, because fine

particles dominate the spectrum, as it is supposed to occur on asteroid's surfaces (Le Bertre & Zellner 1980).

The laboratory diffuse reflectance spectra were obtained in the range of interest (5–12 μm) with a Bruker IFS66v interferometer equipped with a Graseby Specac Mod. Selector accessory at a resolution of 2 cm^{-1}. The optical configuration used to acquire the reflectance spectra is biconical, i.e. the infrared beam is focused onto the sample by means of an ellipsoidal mirror and collected by another ellipsoidal mirror, at 90° from the incident beam. This configuration has the advantage of very high collection efficiency. However, an integrating sphere is the best reflectance attachment to evaluate the particulate emissivity. In fact only absolute directional hemispherical reflectance measurements can be used to predict absolute directional spectral emissivity using Kirchhoff's law. The Graseby reflectance attachment used in our experimental set up is appropriate to determine an accurate curve shape, since it measures diffuse reflectance at 90° to the principal plane. This avoids possible distortion of the Christiansen feature due to preferential forward scattering in the wavelength region that can be a problem when biconical reflectance is measured in the principal plane (e.g. Salisbury et al. 1991a).

All the spectral measurements were performed in vacuum (1 mbar). This prevents changes of the environmental conditions (e.g. atmospheric water vapour and carbon dioxide abundance) during measurements, that could affect the spectral results.

The diffuse reflectance, R, of the particulates is obtained from: $R = R_s/R_r$, where R_s is the diffuse reflectance of the sample and R_r that of the reference. The reference used for diffuse reflectance measurements was finely ground pure CsI powder. Reflectance measurements are an useful tool to derive the emissivity, E, of particulates by using the Kirchhoff's law: $E = 1 - R$. The emissivities obtained in this way have been reported in Fig. 3 and directly compared to the observed spectra divided by the model flux of each asteroid.

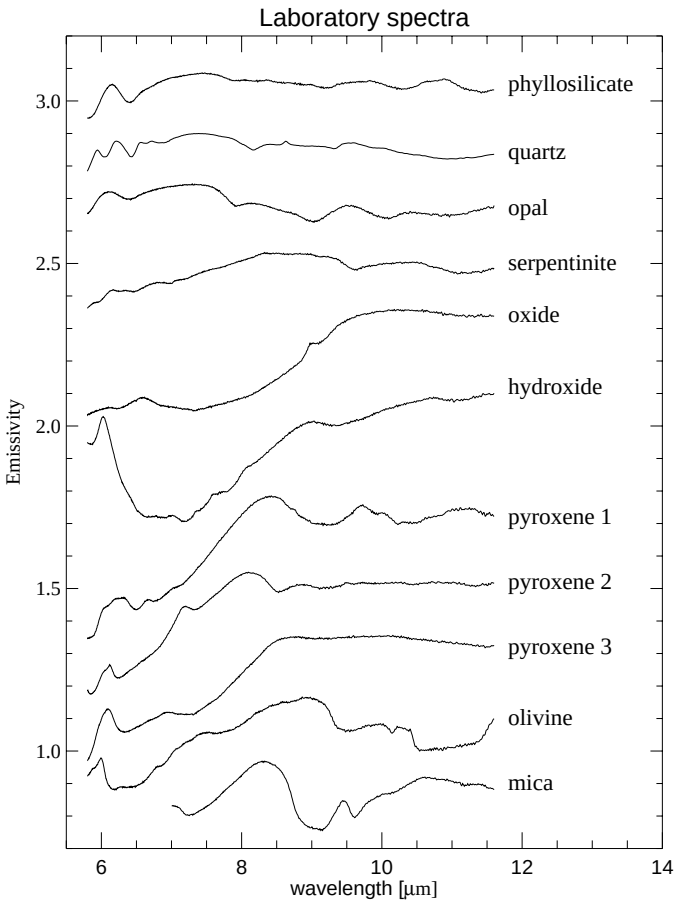

Fig. 3. Emissivity of several mineral samples obtained by laboratory experiments. These spectra are vertically offset for clarity

5. Results

In Figs. 4–8 we plot the relative OBS/MOD obtained for each observed asteroid compared with some mineral analogs.

1 Ceres. Our observations of 1 Ceres were carried out on 14 May 1997. 1 Ceres is the largest asteroid and among the best known objects of the main belt. It is classified as belonging to the G class (Barucci et al. 1987; Tholen 1989). Reflectance spectra of this asteroid, available from the ultraviolet to near infrared region, between 0.3 and 3.6 μm (Feierberg et al. 1981; Bell et al. 1988; Vilas & Gaffey 1989; Jones et al. 1990), suggest a surface composed by a mixture of phyllosilicates and opaque materials which underwent an aqueous alteration process. Lebofsky et al. (1981) and Jones et al. (1990) attributed an absorption feature at about 3.1 μm to a thin water ice component, while King et al. (1992) interpreted the same feature as due to the presence of an ammoniated phyllosilicate. More recently Cohen et al. (1998) obtained KAO observations in the infrared range 5–14 μm and compared their observations with several different materials like ammoniated saponite, tholin and the Murchison meteorite. They matched their KAO observations with an STM expected flux obtained using an η parameter of 1.0 and additional correction factors to get the absolute flux level right. We did not follow the same approach because, without considering these empirical correction factors, it produces an absolute flux too low and no extensive tests with η = 1.0 are so far available. ISO measured Main Belt asteroids with solar phase angles larger than 15° due to Sun viewing constrains. In the picture of the STM, this means a phase angle correction of more than 15%. This implies that a more sophisticated modelling is necessary since most of the groundbased and airborne observations are taken at smaller phase angles, close to opposition, where the STM phase angle corrections are much smaller.

Here we used all the model parameters deduced on this object by Müller & Lagerros (1998) and Müller et al. (1999). The individual observing geometries are calculated automatically from the epochs of the observations.

We compared our spectrum of Ceres with laboratory spectra of several meteorites and materials invoked in previous studies, but we did not find any common features.

As shown in Fig. 4, none of our laboratory spectra exactly matches the observed spectrum, so that we cannot confirm previous interpretation of this asteroid composition. Note however

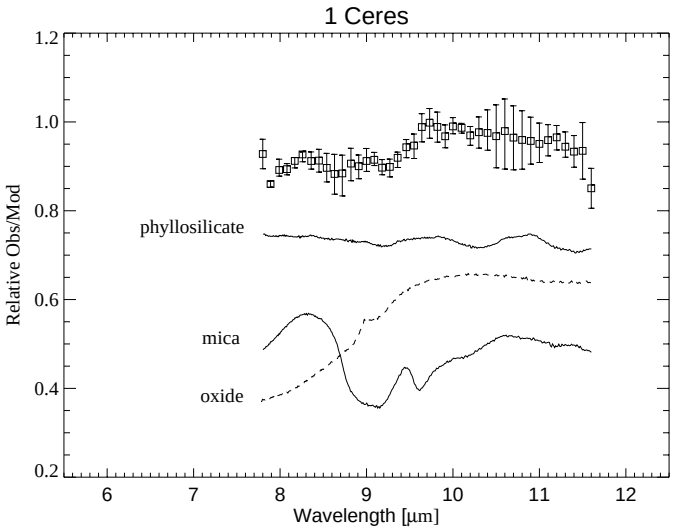

Fig. 4. Relative PHT–S OBS/MOD of 1 Ceres. These spectra are vertically offset for clarity

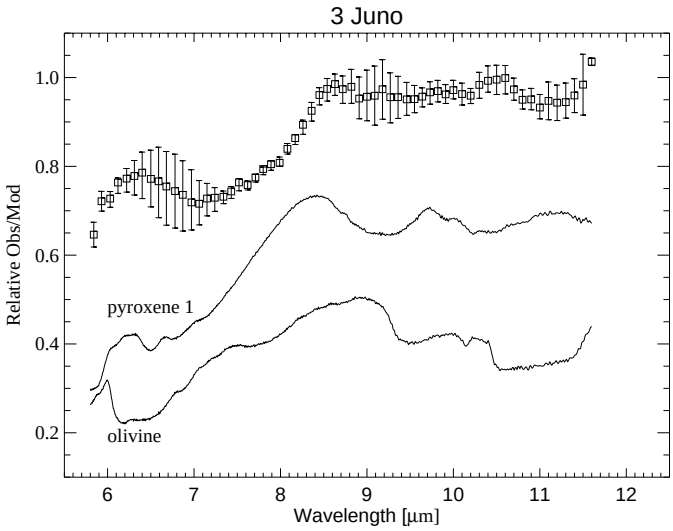

Fig. 6. Relative PHT–S OBS/MOD of 3 Juno. These spectra are vertically offset for clarity

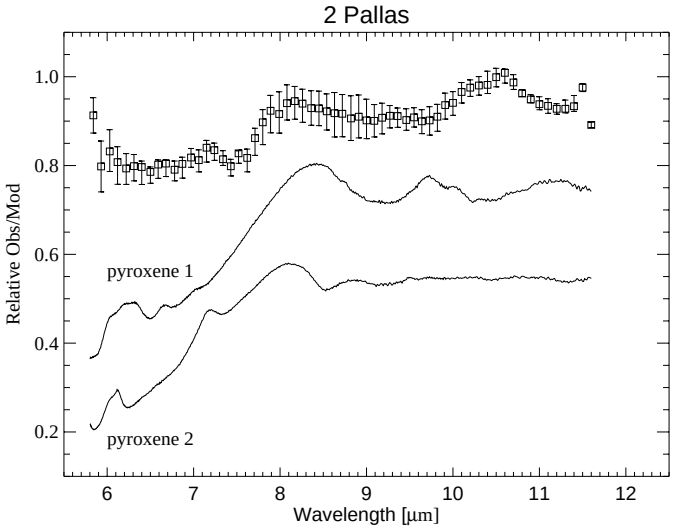

Fig. 5. Relative PHT–S OBS/MOD of 2 Pallas. These spectra are vertically offset for clarity

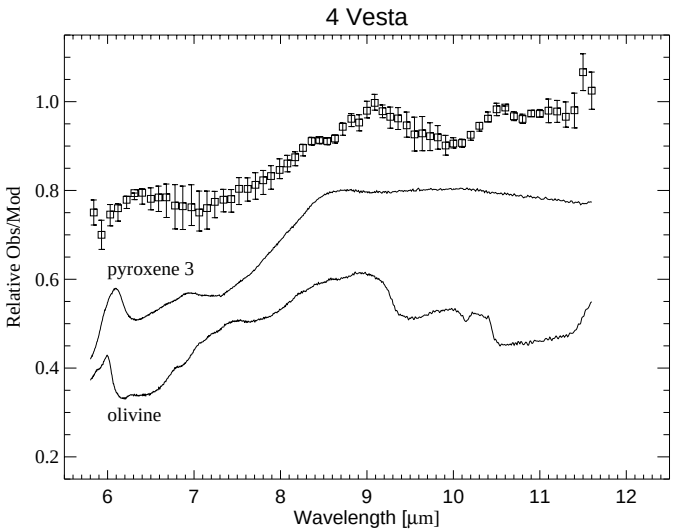

Fig. 7. Relative PHT–S OBS/MOD of 4 Vesta. These spectra are vertically offset for clarity

that the increase of emissivity from 9.2 to 9.7 μm and the constant value longwards is consistent with the spectral behaviour of oxides.

The presence of opaque material aqueous altered (e.g. magnetite or organic material) suggested by several authors (Lebofsky et al. 1981; Feierberg et al. 1981) from reflectance spectroscopy could also not be confirmed here due to the general flat spectra of this material in the analyzed wavelength range.

2 Pallas. Asteroid 2 Pallas was classified by Barucci et al. (1987) and Tholen (1989) as belonging to the B class. Spectra of 2 Pallas in the spectral range 0.3 to 3.6 μm are available in the literature (Gaffey et al. 1993a). Their analysis has suggested the presence on the Pallas surface of Fe-poor phyllosilicates and a significant anhydrous phase.

ISO observations of 2 Pallas were carried out on April 12, 1997 (Fig. 5). The feature at about 8 μm is the Christiansen peak which in the case of Pallas occurs at a shorter wavelength than in most materials and meteorites spectra. The only meteorite with similar position of this emission peak is the aubrite (Salisbury et al. 1991a) which is essentially composed of enstatite. The weak emission peak near 7.2 μm could be explained by a weak overtone/combination tone band seen in aubrite, but not in other meteorites (Salisbury, private communication). Therefore the behavior of the obtained spectrum of Pallas beyond 7.6 μm is compatible with the presence on the surface of pyroxenes. The presence of these minerals on the surface of the asteroid is consistent with its taxonomic classification. As suggested by Salisbury (private communication), the structure at about 10.5 μm is consistent with water ice (Salisbury et al. 1994).

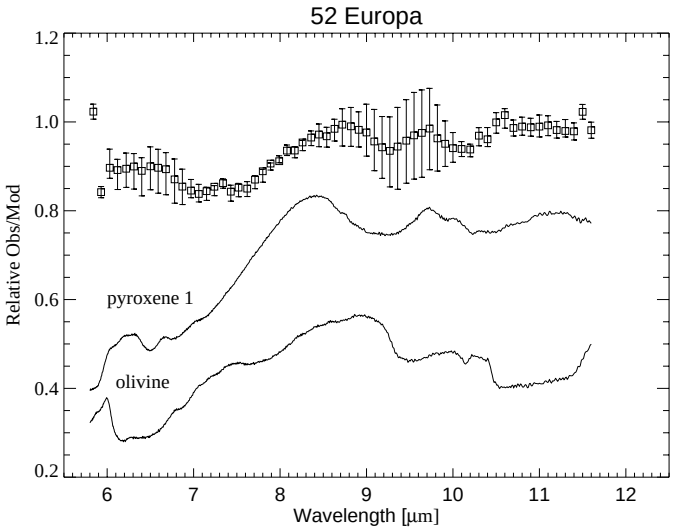

Fig. 8. Relative PHT–S OBS/MOD of 52 Europa. These spectra are vertically offset for clarity

3 Juno. Asteroid 3 Juno was observed on 7 Dec. 1996. The ratio between the observed flux and the expected TPM flux (Fig. 6) shows a large feature between 8 and 11.5 μm whose behaviour is consistent with the ordinary chondrite spectra reported by Salisbury et al. (1991a). This hypothetical surface composition is in agreement with the previous classification (Gaffey et al. 1993b) in which 3 Juno belongs to the S(IV) class. The position of the maximum at about 8.6 μm is intermediate between the Christiansen peak of pyroxenes and olivines and may be due to a mixture of these two minerals. In addition the structure at 6.3 μm seems to be reproduced by the "pyroxene 1".

4 Vesta. Reflectance spectra of asteroid 4 Vesta (V-type) up to 2.5 μm, available in the literature, suggest a surface composition given by a mixture of olivine, pyroxenes and feldspar and a strong similarity with basaltic achondrite meteorites (eucrites, howardites and diogenites). Moreover, as very different spectra have been obtained in correspondence to different rotational phases, it is widely believed that Vesta has a variety of basaltic rocks on its surface (Cochran & Vilas 1998; Lebofsky et al. 1998). Recently HST observations showed the presence of a large crater on the surface (Thomas et al. 1997b).

Vesta was observed by ISO on June 13 1997. The obtained spectrum is shown in Fig. 7. The comparison between the obtained spectrum and those carried out in laboratory for eucrite, howardite and diogenite meteorites (Salisbury et al. 1991a) does not show any common feature and/or continuum component, while the observed structure around 9.1 μm are best matched by the olivines. The presence of augite (high-calcium), suggested by Cochran & Vilas (1998) on the basis of the analysis of a structure centred at 0.5 μm, cannot be confirmed.

52 Europa. Asteroid 52 Europa was classified by Barucci et al. (1987) and Tholen (1989) as belonging to the C class.

Europa was observed by PHT–S on November 16, 1997. The obtained spectrum, shown in Fig. 8, is consistent with that one of carbonaceous chondrite meteorites as reported in Salisbury et al. (1991a). The spectral behaviour between 8 and 11 μm suggests the presence on the surface of a mixture of pyroxenes and olivines. The 8.8 μm maximum seems to be consistent with the Christiansen peak of olivine which occurs at a distinctively long wavelength. At longer wavelengths, olivine and pyroxene exhibit two major reststrahlen bands separated by a band gap which seem to be consistent with our spectrum of Europa even though the error bars in this region are high.

Note that, as opposed to the other asteroids, the TPM for Europa underestimated the absolute flux by as much as 35%. This may suggest a too small input diameter and/or unusually large roughness for this object. Our input diameter is taken from the IRAS catalogue (Tedesco et al. 1992). From occultation measurements Dunham (1983) derived a $2a$ value of 278 ± 14 km, which is even smaller than the IRAS one.

6. Conclusion

In this paper we presented observations of asteroids performed by the ISO satellite with the PHT–S instrument. Black-body and STM sub-solar temperatures were determined for all the observed asteroids. More importantly the observed fluxes have been modelled using an advanced Thermo-Physical Model.

We have been able to match the full PHT–S measurements producing expected fluxes which, in general, fit the observed ones, within the given uncertainties. PHT–S data alone are not sufficient to improve TPM input parameters like thermal inertia or beaming. Only in combination with additional data it will be possible to enhance the accuracy of the existing values.

The obtained spectra have been compared with the emissivity of meteorites and minerals available in literature, and laboratory spectra of a selected sample of minerals have been performed to interpret the obtained spectral features. All the ISO spectra show bands from 8 to 11 μm which have been interpreted as due to the presence of different silicates. As suggested by Salisbury (private communication) the narrow feature at about 10.5 μm clearly detected in 2 Pallas spectrum and hinted in some of the other ones, may be related to the presence of water ice on the surface. If confirmed, this is surprising and suggests the existence of renewal mechanisms. In spite of the limited wavelength range, the low level of spectral features and the difficulties in interpreting the surface composition of asteroids, several specific minerals are tentatively identified.

Acknowledgements. The authors are grateful to Anders Erikson for his input on shape and pole asteroid determinations. We also thank Gian Carlo Parodi and Stephane Erard for helpful discussions regarding the mineralogy of the objects. We would like to express our thanks to Johan Lagerros and especially to John Salisbury for his suggestions and very helpful comments.

References

Barucci M.A., Capria M.T., Coradini A., et al., 1987, Icarus 72, 304

Barucci M.A., Crovisier J., Doressoundiram A., et al., 1997, ESA SP–419, 251
Bell J.F., Owensby P.D., Hawke B.R., et al., 1988, Lunar. Planet. Sci. 19, 57
Cochran A.L., Vilas F., 1998, Icarus 134, 207
Cohen M., Witteborn F.C., Carbon D.F., et al., 1992, AJ 104, 245
Cohen M., Witteborn F.C., Roush T., et al., 1998, AJ 115, 1671
Cohen M., Walker R.G., Carter B., et al., 1999, AJ 117, 1864
Dotto E., Barucci M.A., Crovisier J., et al., 1999, ESA SP–427, 165
Drummond J.D., Fugate R.Q., Christou J.C., et al., 1998, Icarus 132, 80
Dunham D.W., 1983, OCC.NEWSL. 3, 76
Feierberg M.A., Lebofsky L.A., Larson H.P., 1981, Geochim. Cosmochim. Acta 45, 971
Gabriel C., Acosta-Pulido J.A., Heinrichsen I., et al., 1997, In: Hunt G., Payne H. (eds.) ASP Conf. Ser. 125, Astronomical Data Analysis Software and Systems, VI, p. 108
Gaffey M.J., Burbine T.H., Binzel R.P., 1993a, Meteoritics 28, 161
Gaffey M.J., Burbine T.H., Thomas H., et al., 1993b Icarus 106, 573
Hammersley P., Jourdain de Muizon M., Kessler M.F., et al., 1998 A&AS 128, 207
Jämsä S., Peltoniemi J.I., Lumme K., 1993, A&AS 271, 319
Jones T.D., Lebofsky L.A., Lewis J.S., et al., 1990, Icarus 88, 172
Kessler M.F., Steinz J.A., Anderegg M.E., et al., 1996, A&A 315, L27
King T.V.V., Ckaek R.N., Calvin W.M., et al., 1992 Science 255, 1551
Klaas U., Acosta-Pulido J.A., Ábrahám P., et al., 1997, ESA SP–419, 113
Lagerros J.S.V., 1996, A&A 310, 1011
Lagerros J.S.V., 1997, A&A 325, 1226
Lagerros J.S.V., 1998, A&A 332, 1123
Le Bertre T., Zellner B., 1980, Icarus 43, 172
Lebofsky L.A., Spencer J.R., 1989, in Asteroids II (eds..P. Binzel., T. Gehrels and M.S. Matthews) Univ. of Arizona Press. Tucson, 128
Lebofsky L.A., Feierberg M.A., Tokunaga A.T., et al., 1981, Icarus 48, 453
Lebofsky L.A., McCarthy D., Hege E.K., et al., 1998, BAAS 30, 709
Lemke D., Klaas U., Abolins J., et al., 1996, A&A 315, L64
Magnusson P., 1986, Icarus 68, 1
Merline W.J., Stern S.A., Binzel R.P., et al., 1996, BAAS XXVIII, 1025
Michalowski T., Velichko F.P., Di Martino M., et al., 1995, Icarus 118, 292
Millis R.L., Wasserman L.H., Franz O.G., et al., 1987, Icarus 72, 507
Müller T.G., 1997, Ph.D. thesis, Ruprecht-Karls-Universität, Heidelberg (D)
Müller T.G., Lagerros J.S.V., 1998, A&A 338, 340
Müller T.G., Lagerros J.S.V., Burgdorf M., et al., 1999, ESA SP–427, 141
Saint-Pé O., Combes M., Rigaut F., 1993, Icarus 105, 271
Salisbury J.W., Wald A.E., 1992, Icarus 96, 121
Salisbury J.W., D'Aria D.M., Jarosewich E., 1991a, Icarus 92, 280
Salisbury J.W., Walter L.S., Vergo N., et al., 1991b, Infrared (2.1–25 μm) spectra of minerals, Baltimore: Johns Hopkins Univ. Press.
Salisbury J.W., D'Aria D.M., Wald A., 1994, JGR 99, 24,235
Tedesco E.F., Veeder G.J., Fowler J.W., et al., 1992, The IRAS Minor Planet Survey, Phillips Laboratory
Tholen D.J., 1989, In: Binzel R.P., Gehrels T., Matthews M.S. (eds.) Asteroids II, Univ. of Arizona Press. Tucson, p. 1139
Thomas P.C., Binzel R.P., Gaffey M.J., et al., 1997a, Icarus 128, 95
Thomas P.C., Binzel R.P., Gaffey M.J., et al., 1997b, Science 277, 1492
Thompson J.L., Salisbury J.W., 1993, Remote Sensing of Environment 45, 1
Vilas F., Gaffey M.J., 1989, Science 246, 790
Witteborn F.C., Cohen M., Bregman J.D., et al., 1995, In: Haas M.R., Davidson J.A., Erickson E.F. (eds.), ASP Conf. Ser. 73, Airborne Astronomy Symposium of the Galactic Ecosystem, ASP, San Francisco, p. 573